

the chiral quantum numbers of a mass term for the  $\eta$  particle. Comparison with the actual value of the  $\eta$  mass is not yet possible because of the infrared divergences in that theory.

The author would like to thank S. Coleman, R. Jackiw, S. L. Glashow, and all other physicists of the Harvard theory group for discussions.

*Note added.*—In Eq. (22) the isospin indices have been suppressed. The isospin structure of this expression, however, is more complicated than the compact notation suggests. There is also a power of the coupling constant  $g$  in front of the exponent. The full details will be published soon.

\*Work supported in part by the National Science Found-

dation under Grant No. MPS75-20427.

†On leave from the University of Utrecht, Utrecht, The Netherlands.

<sup>1</sup>A. A. Belavin *et al.*, Phys. Lett. **59B**, 85 (1975).

<sup>2</sup>The term "instanton" has been occasionally used elsewhere, and is used in Fig. 1 here.

<sup>3</sup>J. S. Bell and R. Jackiw, Nuovo Cimento **60A**, 47 (1969); S. L. Adler, Phys. Rev. **117**, 2426 (1969).

<sup>4</sup>L. D. Faddeev and V. N. Popov, Phys. Lett. **25B**, 29 (1967); G. 't Hooft and M. Veltman, Nucl. Phys. **B50**, 318 (1972).

<sup>5</sup>J. L. Gervais and B. Sakita, Phys. Rev. D **11**, 2943 (1975); E. Tomboulis, Phys. Rev. D **12**, 1678 (1975).

<sup>6</sup>J. Honerkamp, Nucl. Phys. **B48**, 269 (1972), and in *Renormalization of Yang-Mills Fields and Applications to Particle Physics, Marseille, 19-23 June 1972*, edited by C. P. Korthals Altes (Centre de Physique Théorique, Centre Nationale de la Recherche Scientifique, Marseille, 1972).

<sup>7</sup>R. Jackiw and C. Rebbi, Phys. Rev. **13**, 3398 (1976).

## Evidence for Primordial Superheavy Elements\*

R. V. Gentry†

*Chemistry Division, Oak Ridge National Laboratory, Oak Ridge, Tennessee 37830*

and

T. A. Cahill

*Department of Physics and the Crocker Nuclear Laboratory, University of California, Davis, California 95616, and Department of Oceanography and Physics, ‡ Florida State University, Tallahassee, Florida 32306*

and

N. R. Fletcher, H. C. Kaufmann, L. R. Medsker, and J. W. Nelson

*Department of Physics, Florida State University, Tallahassee, Florida 32306*

and

R. G. Flocchini

*Department of Physics and Crocker Nuclear Laboratory, University of California, Davis, California 95616*  
(Received 16 June 1976)

Accepted without review at the request of Alexander Zucker under policy announced 26 April 1976

Microscopic crystalline monazite inclusions showing giant halo formation in biotite mica have been analyzed by the method of proton-induced x-ray emission. The observed x-ray energy spectra are best explained by the presence of a number of superheavy elements.

Radiation damage induced by alpha-particle decay of uranium and thorium isotopes and daughter products can generate spherical halos that image the known energies of the alpha groups when such materials are contained in microscopic inclusions in transparent materials such as mica.<sup>1</sup> While intensive studies of giant and other halos in certain micas<sup>1</sup> suggest a chemical origin for some,

giant halos (GH) have been found which exhibit three-dimensional structure. This implies a radioactive origin, in which case the halo radii would require  $\alpha$  energies up to about 14 MeV.

This work reports recent investigations of normal uranium/thorium halos and giant halos through the use of ion-induced x-ray analysis with low-energy proton beams.<sup>2-4</sup> The experiment was de-

signed around detection of  $L$  x rays from elements between  $Z = 105$  and  $Z = 134$ , as an x-ray window exists in the spectrum between the last  $L$  transitions of uranium, 21.54 keV, and the first  $K$  transitions of the rare earths, 33.03 keV, as shown in Fig. 1. The use of  $L$  transitions is also advantageous because the energies can be accurately predicted and the cross sections for proton-induced ionization are large.

Protons of 4.7 and 5.7 MeV from the Florida State University tandem Van de Graaff accelerator were prepared in beams of effective diameter of about  $30 \mu\text{m}$  through the use of quadrupole magnets and collimation.<sup>5</sup> A Si(Li) x-ray detector was used, with energy calibration achieved through the use of standard sources, known elemental targets, and known elements occurring in the inclusions. Stability of  $\pm 9$  eV was maintained, while absolute accuracy was maintained to  $\pm 20$  eV. The entire system has undergone numerous validations of precision and absolute accuracy.<sup>6</sup>

Runs were performed on six inclusions with giant halos, five inclusions with uranium/thorium halos, biotite mica foils, two giant halos with inclusions removed, and numerous thin-foil standards of relevant elements. While test foils pro-

vided useful confirmatory information, the most severe tests involved comparison of the inclusions without giant halos with those that possessed them, as these inclusions were very similar in composition and should possess similar x-ray and gamma-ray structure (see Fig. 1). Analysis for all elements, phosphorus and heavier, in both of these inclusions and others, has provided qualitative confirmation of elemental similarities in all inclusions studied to date.

Examination of the spectral region from 22 to 31 keV reveals systematic differences between the GH inclusions and the U/Th inclusions. While this region is always structureless for U/Th inclusions, x-ray peaks appear in spectra from GH inclusions. Figure 2 shows comparison between the three inclusions from mica chip 19. In (a), spectra from inclusions 19B (U/Th halo) and 19D (GH) are presented, as is a smoothed background derived from inclusion 19A. All spectra have been normalized to equal yields of La  $K\alpha$  x rays. While the smoothed background and the spectrum from inclusion 19B are statistically equivalent, structure is apparent in the spectrum from inclusion 19D. Locations of  $K\alpha_1$  and  $K\beta_1$  x rays from known elements<sup>7</sup> and predictions<sup>8</sup> for  $L\alpha_1$ ,  $L\beta_1$ , and  $L\beta_2$  x rays from superheavy elements are shown in Fig. 2(b). Figure 2(c) shows the spectrum of the U/Th inclusion 19B after subtraction of a standard smoothed background derived from inclusion 19A, normalized to the spectrum from inclusion 19A shown in Fig. 2(d). In Fig. 2(e), a similar subtracted spectrum is shown for inclusion 19D.

Effects associated with x-ray detection (sum peaks, escape peaks, Compton edges, etc.) and atomic processes (satellite lines from multiple vacancy formation, radiative Auger emission,<sup>9</sup> etc.) were investigated. All spectrum defects associated with x-ray detection are negligible, while any significant atomic and nuclear process should be equally observed using either type of inclusion.

Searches, both experimental and theoretical, for gamma rays which could explain the structure in the spectra from GH inclusions have been negative. Careful consideration was given to all known target components by means of runs on foil targets and U/Th inclusions.

All statistically significant peaks were considered in the region between 22 and 31 keV. Peak locations were derived from Gaussian fits with fixed, measured widths for singlet lines and convoluted pairs for unresolved  $K\alpha_{1,2}$  doublets. Re-

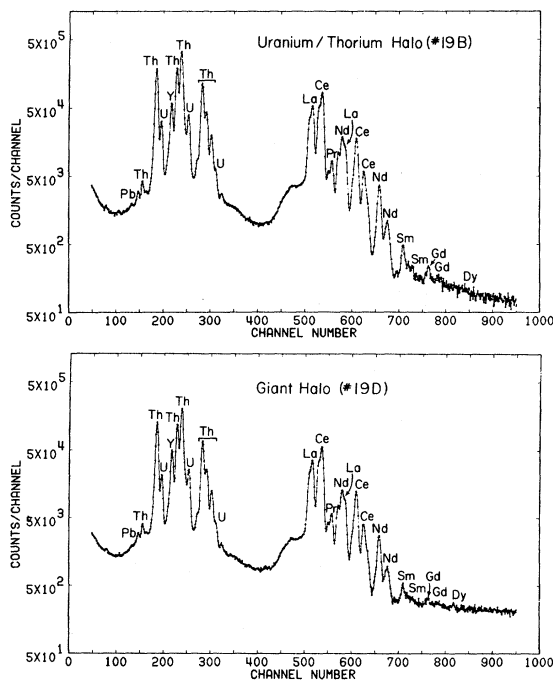


FIG. 1. X-ray pulse-height spectra from the uranium/thorium inclusion 19B and from giant-halo inclusion 19D. The x-ray "window" is shown in the channel number region 330 to 500.

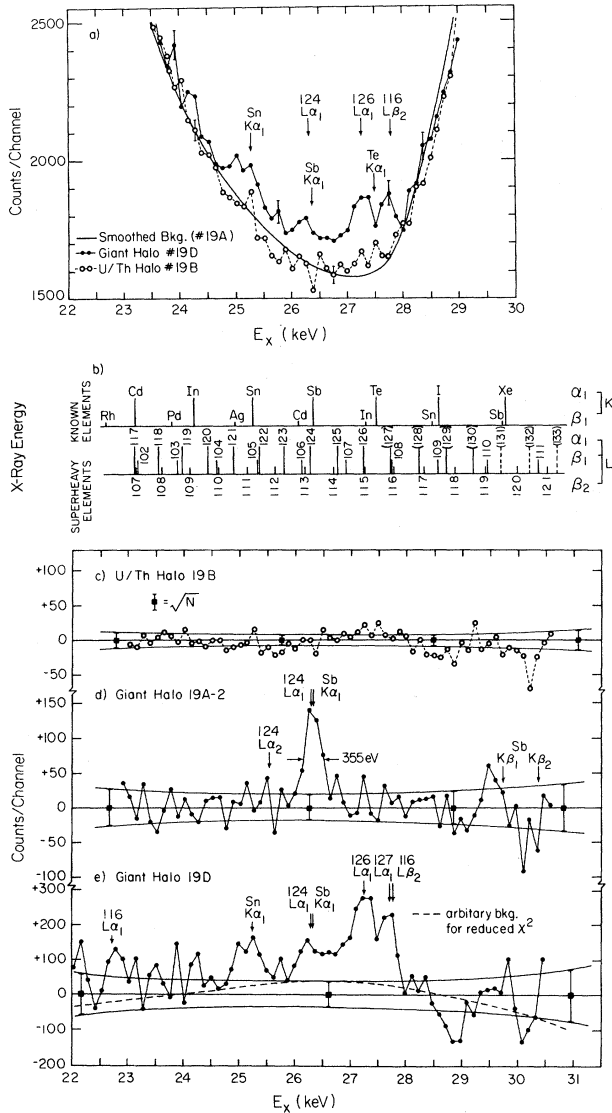


FIG. 2. Comparison of x-ray energy spectra in the window region. The spectra from Fig. 1 are shown in (a). The smoothed background shown in (a) was subtracted, after normalization, to obtain the difference spectra of (c), (d), and (e).

sults are given in Table I including an additional inclusion, GH15.

Evidence for or against a potential elemental source fall into three categories: (a) absolute and relative energy differences between observed and known or predicted lines; (b) intensity ratios, known or predicted,<sup>10,11</sup> between several transitions arising from a given element; and (c) the value of  $\chi^2$  derived from fits to known and predicted transitions using known widths and shapes.

The evidence for the presence of element 126 generates a high level of confidence. The struc-

TABLE I. Summary of x-ray data.

Peak	$E_x$ (eV)	$N_x$ (counts)	$\Delta N_x$ (s) <sup>a</sup>	$\Delta N_x$ (h) <sup>b</sup>	$\chi^2$ (bkgd) outside of peaks
<b>U/Th halo 19B</b>					
None					1.09/pt.
<b>Giant halo 15</b>					
1	27 227 ± 30	168	± 44	± 20	0.91/pt.
<b>Giant halo 19A-2</b>					
1	26 323 ± 20	526	± 44	± 40	0.82/pt.
<b>Giant halo 19D</b>					
1	22 773 ± 40	572	± 138	-114 +345	1.30/pt.
2	25 210 ± 50	370	± 95	± 60	
3	26 261 ± 50	360	± 90	± 50	
4	27 266 ± 30	928	± 90	± 50	
5	27 733 ± 40	420	± 90	± 100	

<sup>a</sup>Statistical error  $\sqrt{N_B}$  in  $N_x$ , where  $N_B$  is background integrated under peak to  $\pm 0.1$  peak maximum.

<sup>b</sup>Variance in  $N_x$  due to displacement of statistical background fit adequate to double background  $\chi^2$  within  $\pm 4$  peak widths (approximately).

ture near 27 250 eV is seen in five out of the six giant halos, and closely coincides with the predicted location of the 126  $L\alpha_1$  transition. In the spectrum of GH15, the difference between observed and predicted energies is  $+26 \pm 58$  eV, while in GH19D, it is  $-13 \pm 58$  eV. Its full width at one-half-peak maximum (FWHM) is close to the observed width of singlet lines at this energy, 350 eV, and  $\chi^2$  fits are good, 1.23/pt. for GH19D and 0.31/pt. for GH15. Weak structure is seen close to the predicted location of the 126  $L\alpha_2$  line in GH15, with an approximately correct intensity ratio. Alternative explanations of the structure are improbable. The In  $K\beta_1$  transition can be evaluated through the presence or absence of the stronger In  $K\alpha$  transitions, and no more than 5% of the observed strength can thus be explained. A Te  $K\alpha$  doublet would have an energy well displaced from the observed peak,  $+173 \pm 32$  eV in GH15 and  $+146 \pm 32$  eV in GH19D, while its distinctive peak shape results in poorer  $\chi^2$  fits, such as 2.45/pt. in GH19D and 0.92/pt. in GH15. At the location predicted for the Te  $K\beta_1$  line, no counts are observed in any of the inclusions. (Analyses of bulk monazites from the same ore body by spark-source mass spectrometry<sup>12</sup> indicate the absence of tellurium to  $< 2$  ppm.) Possible assignment of 27 250 eV structure to 115  $L\beta_2$  is disallowed by the absence of the stronger 115  $L\alpha_1$

at its predicted location.

The line at 27.73 keV can be attributed to elements 116 ( $L\beta_2$ ) or 127 ( $L\alpha_1$ ). The evidence for the presence of element 116 is based upon the simultaneous presence of two transitions, 116  $L\alpha_1$  and 116  $L\beta_2$ , each within one standard error of its predicted energy (Fig. 2). Each line closely coincides in FWHM and peak shape with a singlet x ray,  $\chi^2 = 0.6/\text{pt.}$  and  $1.12/\text{pt.}$ , respectively, in GH19D. However the intensity ratio is a factor of 4 away from predicted values, although background subtraction questions make such calculations difficult. A preferable alternative for the 27.73-keV line is the  $L\alpha_1$  transition in 127. This provides a better  $\chi^2$  for the peak,  $0.56/\text{pt.}$ , and considerable 127 content would bring the 116  $L\alpha_1/L\beta_2$  intensity ratio into accord. Alternative explanations for a major contribution to the line at 27.73 keV are improbable. The Rh  $K\beta_1$  could provide strength at the 116  $L\alpha_1$  location, but absence of the stronger Rh  $K\alpha$  lines limits contributions from this source to a few percent. The Te  $K\alpha$  doublet is well displaced from the 116/127 location,  $-321 \pm 42$  eV, the Te  $K\beta_1$  is not observed ( $-2 \pm 115$  counts), and its distinctive peak shape is not in accord with the Gaussian shape of the line,  $\chi^2 = 2.8/\text{pt.}$

The evidence for the presence of element 124 is less strong than that for 126 because of the possible presence of the  $K\alpha_{1,2}$  line of Sb. Structure at the location 124/Sb, near 26 300 eV, is seen in three of the six GH inclusions and never in the five U/Th inclusions. The energy predicted for the 124  $L\alpha_1$  provides a good match to the observed energies,  $-15 \pm 54$  eV for spectrum GH19A-2, and the observed FWHM, 355 eV, is close to that of a singlet x ray at that energy, 350 eV. The  $\chi^2$  for a fit to the 124  $L\alpha_1$  line is  $0.5/\text{pt.}$  At the predicted location of the 124  $L\alpha_2$  line, excess counts are present in GH19A-2,  $41 \pm 40$  counts versus a predicted  $50 \pm 5$  counts.

The Sb  $K\alpha_{1,2}$  doublet matches the energy of the line in GH19A-2 reasonably well,  $-47 \pm 23$  eV, but the characteristic shape and FWHM of 492 eV result in a poorer  $\chi^2$ ,  $1.78/\text{pt.}$  Weak evidence against the presence of Sb is contained in the absence of the Sb  $K\beta_1$  peak. Sb is not seen in bulk monazites from the same ore body to  $< 2$  ppm, as analyzed by spark-source mass spectrometry,<sup>12</sup> while secondary ion mass spectrometry on other GH inclusions likewise has not indicated any significant amount of this element.<sup>13</sup> Possible explanations of the 124/Sb line by the 106  $L\beta_1$  and/or the 113  $L\beta_2$  suffer from poor agreement in en-

ergy, and the predicted 106  $L\beta_2$  is not observed. The Cd  $K\beta_1$  x ray could provide counts at the location of the 124/Sb line, but absence of the stronger Cd  $K\alpha_1$  line limits such contributions to  $11 \pm 15$  counts in GH19A-2. Weak structure at the location of either the 114  $L\beta_2$  or the 125  $L\alpha_1$  structure is seen in some of the giant-halo inclusions.

Using extrapolated cross sections for ion-excited x rays,<sup>11</sup> the mass of superheavy elements present in monazite inclusions showing giant halos could be as high as several hundred picograms. Improved control of the ion-beam optics should allow more detailed studies to be made of giant-halo inclusions, including those used in the present study, which should confirm or deny the evidence for superheavy elements.

We wish to acknowledge the development of accelerator-based analytical systems without which this work would not have been possible. This was accomplished through the support of the Environmental Research Laboratory of the U. S. Environmental Protection Agency, the Trace Contaminants Section of National Science Foundation/Research Applied to National Needs, and the California Air Resources Board. Advice and encouragement for this project were supplied by O. L. Keller, T. A. Carlson, S. Datz, F. G. Perey, R. L. Hahn, and E. H. Taylor of the Oak Ridge National Laboratory, M. Ahlberg, W. Courtney, R. Davis, J. Fox, D. Gustafson, D. Robson, and J. Winchester at the Florida State University, and R. A. Eldred, University of California, Davis. One of us (TAC) wishes to acknowledge substantial support from the University of California, Davis. Exceptional support was given the project by B. Jensen and Department of Physics mechanical shops, and by the entire crew of the tandem accelerator.

\*Work supported in part by the National Science Foundation Grants No. NSF-PHY-7503767-A01, No. NSF-GU-2616, and No. NSF-DES-23451, and by the U. S. Energy Research and Development Administration under contract with Union Carbide Corp.

†Visiting scientist at Oak Ridge National Laboratory from Columbia Union College, Takoma Park, Md, 20012.

‡Visiting professor.

<sup>1</sup>R. V. Gentry, *Annu. Rev. Nucl. Sci.* **23**, 347 (1973), and *Science* **169**, 670 (1970).

<sup>2</sup>T. B. Johansson, R. Akselsson, and S. A. E. Johansson, *Nucl. Instrum. Methods* **84**, 141 (1970).

<sup>3</sup>T. A. Cahill, in *New Uses of Ion Accelerators*, edited by J. Ziegler (Plenum, New York, 1975), pp. 1-72.

<sup>4</sup>T. B. Johansson, R. E. Van Grieken, J. W. Nelson, and J. W. Winchester, *Anal. Chem.* **47**, 855 (1975).

<sup>5</sup>B. Jensen and J. W. Nelson, *Nucl. Instrum. Methods* **71**, 137 (1971).

<sup>6</sup>D. C. Camp, A. L. van Lehn, J. R. Rhodes, and A. H. Pradzynski, *J. X-Ray Spectrom.* **4**, 123 (1975).

<sup>7</sup>J. A. Bearden and A. F. Burr, *X-Ray Wavelengths and X-Ray Atomic Energy Levels*, U. S. National Bureau of Standards Special Publication No. NSRDS-NBS14 (U.S. GPO, Washington, D.C., 1967).

<sup>8</sup>T. A. Carlson, C. W. Nestor, F. B. Malik, and T. C. Tucker, *Nucl. Phys.* **A135**, 57 (1969); C. C. Lu, F. B. Malik, and T. A. Carlson, *Nucl. Phys.* **A175**, 289

(1971).

<sup>9</sup>G. Presser, *Phys. Lett.* **56A**, 273 (1976).

<sup>10</sup>E. Storm and H. I. Israel, *Nucl. Data, Sect. A* **7**, 565 (1970); R. Anholt and J. O. Rasmussen, *Phys. Rev. A* **9**, 585 (1974).

<sup>11</sup>R. K. Wyrick and T. A. Cahill, *Phys. Rev. A* **8**, 2288 (1973); R. G. Flocchini, thesis, University of California, Davis, 1974 (unpublished).

<sup>12</sup>J. C. Franklin and L. Landau, private communication.

<sup>13</sup>W. H. Christie and D. H. Smith, private communication; S. S. Cristy and J. F. McLaughlin, private communication.

## Experimental Determination of the Charge Density of the Bond-Forming Electrons in N<sub>2</sub> †

M. Fink, D. Gregory, and P. G. Moore\*

*Physics Department and Electronics Research Center, The University of Texas, Austin, Texas 78712*

(Received 22 April 1976)

High-precision total differential scattering cross sections for 40-keV electrons incident on N<sub>2</sub> have been measured. In order to observe binding effects in the scattering cross sections, the data have been compared to a theoretical set of intensities based on scattering from noninteracting nitrogen atoms placed in the proper geometric relation. The resulting difference function has been Fourier transformed according to the procedures described by Kohl and Bartell. The charge-density-difference map which is the result of this deconvolution process is compared with the Hartree-Fock model.

During the last few years, a new electron diffraction unit utilizing counting techniques has been designed and built at the University of Texas at Austin. The unit was conceptually based on a unit described by Fink and Bonham<sup>1</sup> and by Bonham and Fink<sup>2</sup> and will be described in detail in another publication.<sup>3</sup> Two major improvements have been achieved; the present uncertainty in the scattering angle is  $\pm 2$  arc sec, and the scattered intensity is recorded with an average of 0.1%. The resulting data for 40-keV electrons incident on N<sub>2</sub> are of sufficient accuracy to warrant, for the first time, a critical comparison between theoretical predictions of bonding-electron rearrangement in molecules and the corresponding experimental results. An experimental charge-density map showing this bonding-electron rearrangement has been constructed, and is compared to the Hartree-Fock model (which appears

to be inadequate to describe certain features found in the experimental charge-density map). Even if the necessary assumptions in the development of the charge-density map prove to be faulty, future theoretical charge densities, when transformed to scattering cross sections, can be directly compared to the present data.

Experimental scattered intensities, generally expressed in terms of the Rutherford cross section as  $s^4 I(s)$ , may be compared to theory by subtracting the scattered intensities predicted by the independent-atom model (IAM), i.e., the scattering from a molecule made of noninteracting atoms in the proper geometric arrangement with vibrational and rotational averaging taken into account. The difference between the experiment and the model calculation is called a  $\Delta\sigma$  function and can be expressed theoretically for N<sub>2</sub> in terms of the atomic charge densities as

$$\Delta\sigma(s) = \frac{1}{16}(\pi a_0^2) s^4 (I_{\text{exp}} - I_{\text{theor}}) = -2Z \int_0^\infty r^2 \Delta\rho(r) j_0(sr) dr + \int_0^\infty r^2 \Delta\rho_e(r) j_0(sr) dr, \quad (1)$$

where  $s = (4\pi/\lambda) \sin\theta/2$  is the momentum transfer,  $Z$  is the atomic number, and  $\Delta\rho(r)$  and  $\Delta\rho_e(r)$  are the radial parts of, respectively, the electron-nuclear and electron-electron charge-difference functions reflecting the rearrangement of the charge densities when the chemical bond is formed.

The transformation from the momentum space in which the cross section is determined to real space